

Article

Not peer-reviewed version

---

# Transmission Spectroscopy Along the Transit of Venus: A Proxy for Exoplanets Atmospheric Characterization

---

Alexandre Baptista Branco , [Pedro Machado](#) <sup>\*</sup> , Olivier Demangeon , [Sarah Amelia Jaeggli](#) , [Thomas Widemann](#) , [Paolo Tanga](#)

Posted Date: 11 July 2024

doi: 10.20944/preprints202407.0928.v1

Keywords: Venus; Solar Transit; High-resolution transmission spectroscopy; Radiative transfer; Cross-correlation; Carbon dioxide; Carbon monoxide; Ozone; Venus-like exoplanets








Preprints.org is a free multidiscipline platform providing preprint service that is dedicated to making early versions of research outputs permanently available and citable. Preprints posted at Preprints.org appear in Web of Science, Crossref, Google Scholar, Scilit, Europe PMC.

Copyright: This is an open access article distributed under the Creative Commons Attribution License which permits unrestricted use, distribution, and reproduction in any medium, provided the original work is properly cited.

## Article

# Transmission Spectroscopy Along the Transit of Venus: A Proxy for Exoplanets Atmospheric Characterization

Alexandre Branco <sup>1,2</sup>, Pedro Machado <sup>1,2,\*</sup> , Olivier Demangeon <sup>3,4</sup> , Sarah Jaeggli <sup>5</sup> , Thomas Widemann <sup>6,7</sup>  and Paolo Tanga <sup>8</sup> 

<sup>1</sup> Institute of Astrophysics and Space Sciences, Observatório Astronómico de Lisboa, Ed. Leste, Tapada da Ajuda, 1349-018 Lisbon, Portugal

<sup>2</sup> Faculdade de Ciências, Universidade de Lisboa, Campo Grande 016, Lisboa, 1749-016, Portugal

<sup>3</sup> Institute of Astrophysics and Space Sciences, Universidade do Porto, CAUP, Rua das Estrelas, 4150-762 Porto, Portugal

<sup>4</sup> Departamento de Física e Astronomia, Faculdade de Ciências, Universidade do Porto, Rua do Campo Alegre, 4169-007 Porto, Portugal

<sup>5</sup> National Solar Observatory, 22 Ohia Ku Street, Pukalani, HI 96768, USA

<sup>6</sup> LESIA - UMR CNRS 8019 - Laboratoire d'Études Spatiales et d'Instrumentation en Astrophysique, Observatoire de Paris, CNRS, UPMC, Université Paris-Diderot, 5 place Jules Janssen, 92195 Meudon, France

<sup>7</sup> Université Versailles St-Quentin - DYPAC EA 2449, 47 boulevard Vauban, 78280 Guyancourt, France

<sup>8</sup> Université Côte d'Azur, Observatoire de la Côte d'Azur, CNRS, Laboratoire Lagrange UMR7293, Nice, France

\* Correspondence: pmmachado@fc.ul.pt

**Abstract:** We present an analysis of high-resolution, near-infrared (NIR) spectra relative to the solar transit of Venus of 5-6 June 2012, as observed with the Facility Infrared Spectropolarimeter (FIRS) at the Dunn Solar Telescope in New Mexico. These observations offer the unique opportunity to probe the upper layers (between ~84 and 150 km in altitude) of a thick, CO<sub>2</sub>-dominated atmosphere with the transmission spectroscopy technique – a proxy for future studies of highly-irradiated atmospheres of Earth-sized exoplanets. We were able to visually identify absorption lines from the two most abundant CO<sub>2</sub> isotopologues, and from the main isotopologue of CO in the retrieved spectrum of Venus. Furthermore, we perform a cross-correlation analysis of the transmission spectrum using transmission templates generated with petitRADTRANS. With the cross-correlation technique, it was possible to confirm detections of both CO<sub>2</sub> isotopologues and CO. Additionally, we retrieve a cross-correlation signal for O<sub>3</sub> on Venus. We demonstrate the feasibility of high-resolution, ground-based observations to study the chemical inventory of planetary atmospheres, employing techniques commonly used in exoplanet characterization.

**Keywords:** venus; solar transit; high-resolution transmission spectroscopy; radiative transfer; cross-correlation; carbon dioxide; carbon monoxide; ozone; venus-like exoplanets

## 1. Introduction

The transits of Venus across the solar disk represent some of the rarest astronomical phenomena which can be predicted. Historically, these events have a great scientific relevance. In the eighteenth century, they enabled the first detection of the Venusian atmosphere and motivated the first estimates of the absolute scale of the Solar System [1,2]. The transit of Venus of 5-6 June 2012 was the last one of the twenty-first century and it offered a unique opportunity to closely observe a transiting, thick, CO<sub>2</sub>-dominated atmosphere using high-resolution ground-based spectrographs [3].

Several studies have relied on the transmission spectroscopy technique to characterize the atmospheric composition, dynamics and structure of hot giant exoplanets [4–6]. This technique is also being applied to the characterization of increasingly smaller planets, including mini-Neptunes, super-Earths and telluric Earth-sized worlds [7,8]. Nonetheless, a challenging aspect of the

characterization of small, Earth-mass exoplanets arises from their compact atmospheres, with small atmospheric scale heights [9].

As future ground- and space-based observatories (e.g. ELT or ARIEL) aim to characterize potential Earth-analogs, Venus comprises a valuable proxy for an Earth-sized rocky exoplanet. Due to their short orbital periods, Venus-like planets are easier to detect and characterize with the transit method than planets with similar radii but larger orbital distances. Thus, the characterization of nearby, highly irradiated atmospheres, akin to Venus, is likely to initiate the study of Earth-sized planets within the inner edge of the habitable zone [10]. In this context, dedicated observations of Venus solar transits consist of an important test bed to the feasibility of current atmospheric characterization techniques to effectively study exoplanets within this mass range [2,11].

Observations of Venus transits can also help to identify observational discriminants of a Venus-like atmosphere and climate, which can be critical to distinguish between Earth- and Venus-like exoplanets in future observation campaigns. On this regard, the prominent observation of strong carbon dioxide bands (e.g.,  $4.3\ \mu\text{m}$ ) in transmission spectra have been regarded as a good indicator for the presence of a terrestrial atmosphere, nonetheless they appear insufficient to discriminate between a  $\text{CO}_2$ -dominated environment and an atmosphere with trace abundances of this gas [12]. The additional observation of the weaker  $\text{CO}_2$  bands can, however, suggest a higher, Venus-like abundance and allow to differentiate between distinct terrestrial climates [12]. Particularly, near-infrared (NIR) spectral bands (e.g.,  $1.5$ ,  $2.0$  and  $4.8\ \mu\text{m}$ ) offer the opportunity to observe some of these weaker spectral lines.

In this context, this work presents the analysis of high spectral resolution ( $R \sim 90,000$ ), NIR observations of Venus solar transit of 5-6 June 2012. Particularly, we aimed to retrieve the planetary transmission spectrum from the aureole region of Venus.

The aureole consists of a shining arc of light that is observed along the limb of Venus just before it enters onto or emerges off the solar disk. This optical phenomenon is caused by the diffraction of sun light by aerosols in the mesosphere of Venus above the main cloud deck ( $70\text{--}100\ \text{km}$ ) [1,13]. At these altitudes, the atmosphere of Venus is dominated by  $\text{H}_2\text{SO}_4$ -aerosol particles which form an atmospheric haze [2]. The atmospheric aureole of Venus results from Mie scattering at this high-altitude haze layer.

We complement our study with a cross-correlation analysis of the transmission spectrum here retrieved. The cross-correlation technique is commonly used in the characterization of exoplanetary atmospheres, and it has successfully allowed the detection of atmospheric species in high noise spectra [4,5]. Attending to the high planetary signal intrinsic to our observations, we aimed to address the feasibility of this statistical tool under conditions where spectral absorption lines can be effectively resolved.

## 2. Observations

Observations of the Venus solar transit of 5-6 June 2012 were conducted with the infrared arm of the Facility Infrared Spectropolarimeter (FIRS) at the  $76.2\ \text{cm}$  aperture Dunn Solar Telescope (DST), located at the U.S. National Solar Observatory on Sacramento Peak, New Mexico [14]. The observations were performed using FIRS Fe I  $15648\ \text{\AA}$  mode, which covers a near-infrared wavelength range from  $15624\ \text{\AA}$  to  $15680\ \text{\AA}$ . Combined with a single instrument slit, with a width of  $0.3''$  and height of  $75''$ , this observation mode enabled us to achieve a spectral resolving power of  $R \sim 90\ 000$ . The employed FIRS mode is affected by a Rayleigh limit of  $0.52''$ , however, Venus' apparent diameter during observations was of  $57.8''$ . Hence, this data provides spatially resolved spectra of the Venus disk, following a spatial sampling of  $0.22'' \times 0.15''/\text{pixel}$ .

The FIRS slit was aligned perpendicularly to the transit path and was scanned in the direction of the planet's path across the Sun. This study handles with 295 2-D spectra taken throughout the Venus' passage of the solar limb at ingress. Each 2-D spectrum corresponds to a  $125\ \text{msec}$  exposure with associated values of spectral intensity across 502 spatial pixels and 1018 wavelength bins, with a binning of  $0.055\ \text{\AA}$ . All exposures were individually processed, following bias, dark and flat-field

corrections. For the latter, a master flat-field image was constructed from observations of the solar disk center with spectral lines removed [14]. A solution to the spectral geometry and wavelength was determined based on line fitting in spectra taken with a calibration grid. The spectra were then interpolated to make the spectral and spatial coordinates rectilinear.

### 3. Methodology

#### 3.1. Transmission Spectrum Extraction

To extract the transmission spectrum of Venus we started by reconstructing an intensity raster map [14]. Each 2-D spectrum had its values of spectral intensity averaged across all wavelength bins for each row of spatial pixels. This results in 295 *slices* with an individual averaged value of spectral intensity for each spatial pixel. All *slices* were then stacked next to one another according to the scanning spatial sequence, resulting in the raster map (Figure 1; average intensity represented by a log-scaled color bar). The intensity distribution on the map facilitates the identification of groups of pixels sampling the Sun (showcasing a maximum of intensity towards the right-hand side of the image), as well as the planetary disk blocking a portion of the solar disk between contacts I and II.

The raster map showcases a region of particularly enhanced average spectral intensity surrounding the planetary disk at the centre-top part of the image (between  $X = 110$  and  $210$ , and  $Y = 420$  and  $460$ ). This thin band corresponds to the aureole of Venus' atmosphere. This particular region of the planetary limb was used to extract our planetary transmission spectrum. For that, we started by describing a spatial window around Venus which enveloped the limb. Attending to the apparent diameter of Venus during observations (of  $57.8''$ ) and to the spatial sampling of our data ( $0.22'' \times 0.15''/\text{pixel}$ ), we admitted that the planetary limb comprises the area delimited by two concentric ellipses centered at  $(X,Y) = (190, 265)$ , as illustrated with gray dashed lines in Figure 1.

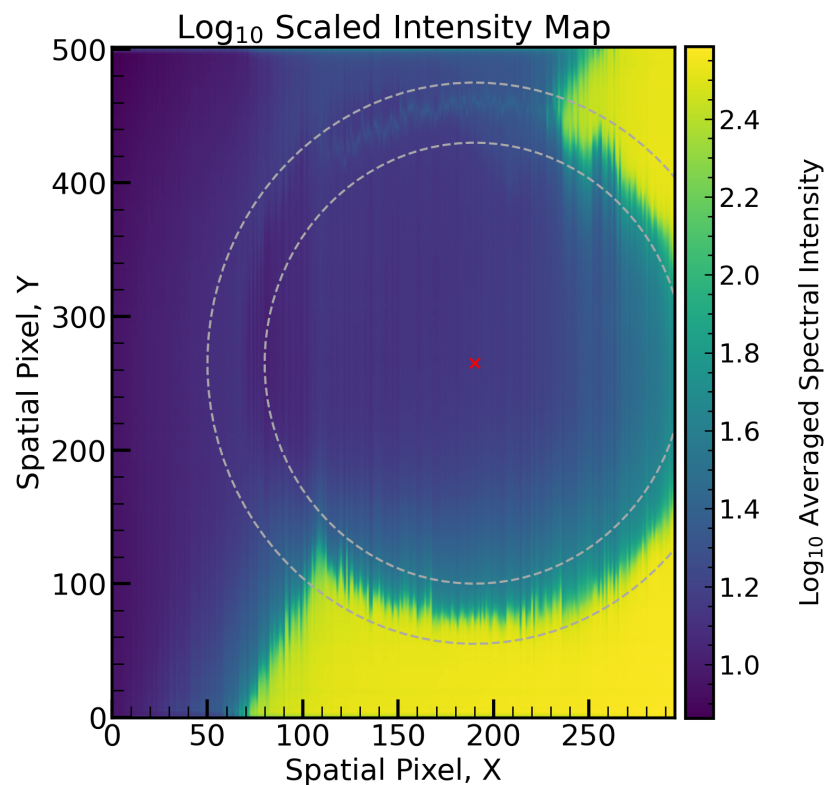


**Figure 1.** Intensity raster map with averaged spectral intensity represented in log-scale. Gray dashed lines delimit the region containing the planetary limb. These represent two concentric ellipses centered at  $(X,Y) = (190, 265)$ , marked with a red cross.

We then reconstructed the intensity raster map for the region between both ellipses in which the aureole signal could be observed, i.e. between  $X = 120$  and  $X = 219$ . All slices were subsequently re-aligned such that the pixels with maximum spectral intensity were at the same vertical position (Figure 2). A spatial window, centered around these high-intensity pixels, was selected with a width of four pixels in order to define our region of interest pertaining the atmospheric aureole. All spectra contained within this area are considered to carry the atmospheric signal of the planet.

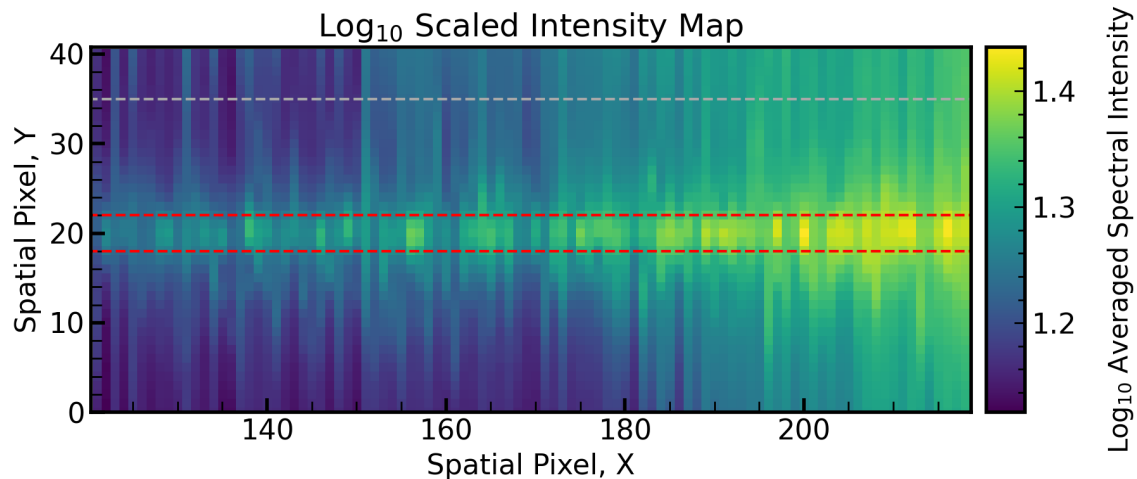


**Figure 2.** Intensity raster map of the aureole region aligned by the highest intensity pixel in each slice, with averaged spectral intensity represented in log-scale. The red dashed lines delimit a 4 pixel tall window of interest, defining the region of interest pertaining the atmospheric aureole. The gray dashed line defines an out-of-interest area separated by 13 pixels from the top of our region of interest and spanning until the top of each slice. Out-of-interest spectra were used to correct for the presence of stray light in aureole spectra.

To account for the presence of stray light contaminating our aureole spectra, we selected an out-of-interest area separated by 13 pixels from the top of our region of interest and spanning until the top of each slice. For each slice, we extracted the corresponding transmission spectrum by averaging the spectra of interest and dividing the result by the average background spectrum from the same slice. We note that this step results in the normalization of our spectra, while also removing the telluric absorption lines [11].

Lastly, we combined all the individual transmission spectra into a unique average spectrum of Venus with a higher signal-to-noise ratio. Consequently, the information about the altitude and the corresponding Doppler-shifts by winds were lost with this step [11].

### 3.2. Atmospheric Transmission Models

In order to perform a cross-correlation analysis of the transmission spectrum of Venus [5], we used the *petitRADTRANS* package [15] to create an atmospheric transmission model for each chemical specie here regarded.

Attending to the chemical abundances estimated for the upper atmosphere of Venus [2,16], we searched for species which could present absorption lines in our wavelength range. Particularly, we aimed to retrieve cross-correlation signals for  $\text{CO}_2$ ,  $\text{CO}$  and  $\text{O}_3$ .

*petitRADTRANS* is a radiative transfer code commonly used to calculate transmission spectra of exoplanetary atmospheres at either low- or high-spectral resolution. Our models were computed at a



resolving power of  $R = 10^6$ , and were subsequently convolved with a Gaussian kernel using `tayph`<sup>1</sup>, so that the spectral resolution could be reduced to match that of FIRS. `petitRADTRANS` takes as input a pressure-temperature (PT) profile, the planetary radius and surface gravity, the mean-molecular weight of the atmosphere and the abundances of the requested species.

Ehrenreich, D.; et al. (2012) [2] calculated a theoretical transmission spectrum of the atmosphere of Venus as it could be observed during the solar transit of June 2012. The lowest altitude in Venus that is possible to be probed with transmission spectroscopy is set by Mie scattering from the high-altitude atmospheric haze, which corresponds to the dominant diffusion regime in Venus’ atmosphere. The lowest altitude probed with our NIR observations should correspond to  $\sim 72$  km, if the atmospheric haze is only composed of mode-1 aerosol particles, and  $\sim 84$  km if mode-2 particles are also included [2].

Following Ehrenreich, D.; et al. (2012) [2], NIR transmission spectroscopy of Venus can sound the atmospheric layers from the top of the cloud deck up to 150 km in altitude. Based on the Venus International Reference Atmosphere (VIRA) [17,18] temperature profile at these altitudes, we chose to approximate the Venus’ PT profile to an isothermal profile with a temperature of 175 K. We adopted atmospheric top and bottom pressures of  $10^{-8}$  and  $10^{-3}$  bars, respectively, for all models except for that of  $^{16}\text{O}_3$ . Attending to the localized vertical distribution of ozone on Venus ( $\sim 90$ -100 km; [19]), we adopted atmospheric top and bottom pressures of  $10^{-6}$  and  $10^{-5}$  bars, respectively, for computing the corresponding transmission model.

The `petitRADTRANS` package has available pre-computed line opacities of  $^{12}\text{C}^{16}\text{O}_2$ ,  $^{12}\text{C}^{16}\text{O}$  and  $^{16}\text{O}_3$ , which we included in our models. We also converted pre-computed line opacities of  $^{13}\text{C}^{16}\text{O}_2$  from the Data Analysis Centre for Exoplanets (DACE) opacity database<sup>2</sup> [20] into the `petitRADTRANS` format, following the procedure described in the code documentation website<sup>3</sup>. For all gases we assumed constant vertical abundance profiles (see Table 1 for the adopted abundances). In Figure A1 we show our transmission templates ready to be used for cross-correlation.

Note that no continuum opacities (e.g., from clouds or aerosols) were included in our transmission models from `petitRADTRANS`. Attending to the altitudes sounded with our observations, the extracted transmission spectrum pertains to an atmospheric layer in which extinction by  $\text{H}_2\text{SO}_4$  cloud particles can essentially be neglected, as this effect is expected to extend up to about 80 km altitude [21–23]. Moreover, Venus Express SPICAV/SOIR observations by Wilquet, V.; et al. (2009) [24] showcased how the extinction coefficient of the atmospheric haze measured at 1553.7 nm decreases to about  $2 \times 10^{-4}$  at 90 km altitude. For larger wavelengths (such as those of our observations), this extinction coefficient should be even smaller, and significantly lower than the  $\text{CO}_2$  absorption coefficient. Hence, haze opacities can also be neglected [11].

**Table 1.** Molecular abundances used in atmospheric transmission models.

Molecule	Volume Mixing Ratio	Reference
$\text{CO}_2$	0.965	[16]
CO	$3.3 \times 10^{-3}$	[16]
$\text{O}_3$	$10^{-6}$	[19]

3.3. Cross-Correlation Analysis

We carried out a cross-correlation analysis using the normalized spectrum of Venus and the transmission templates of each molecular species. The cross-correlation technique enables individual lines in the transmission spectrum to be combined into a unique line profile. This statistical approach

<sup>1</sup> <https://github.com/Hoeijmakers/tayph>  
<sup>2</sup> <https://dace.unige.ch/opacityDatabase/>  
<sup>3</sup> <https://petitradtrans.readthedocs.io>

has been successfully used for the characterization of exoplanetary atmospheres, since it enables the detection of chemical species whose lines would otherwise go unnoticed due to the high noise in the transmission spectrum [5].

We note that during the transit of 5-6 June 2012, Venus was approximately three times closer to the Earth than the Sun. The transit depth can be estimated as the ratio between the angular diameters of the two bodies (57.8'' for Venus and 31.5' for the Sun), which results in 934 ppm [2]. For an Earth-sized exoplanet transiting a Sun-like star, the transit depth would be 75.7 ppm [2].

Hence, these observations offer the opportunity to test the feasibility of the cross-correlation technique with a low noise planetary spectrum, as opposed to the high noise expected in future observations of telluric exoplanets. Nevertheless, we also relied on the cross-correlation analysis to search for species whose absorption lines could have gone unnoticed during the visual inspection of the transmission spectrum (e.g., faint spectral features).

We computed the cross-correlation functions (CCFs) using the SciPy cross-correlation tool [25] and we fit Gaussian profiles to the CCFs of the species showing planetary absorption features. We used the lmfit Python package [26] to find the best-fit values and respective uncertainties.

## 4. Results and Discussion

### 4.1. Planetary Transmission Spectrum

The average transmission spectrum of Venus extracted from the region of the atmospheric aureole is shown in Figure 3. Several weak absorption lines were detected upon a visual inspection of the spectrum. Using line positions from the HITRAN (High-Resolution Transmission Molecular Absorption Database; [27]) line database as a reference, it was possible to identify the atmospheric absorption lines as those of  $^{12}\text{C}^{16}\text{O}_2$ ,  $^{13}\text{C}^{16}\text{O}_2$  and  $^{12}\text{C}^{16}\text{O}$  (see Figure 3).

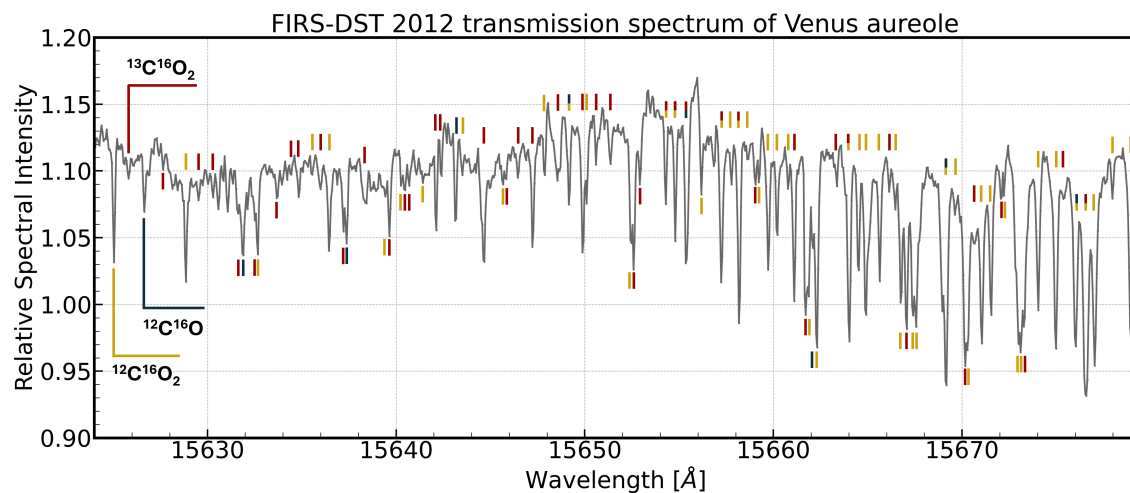


**Figure 3.** Average transmission spectrum of Venus extracted from the atmospheric aureole as observed during the solar transit of 2012. For each slice, an average spectrum of the Venus limb was calculated and divided by an average spectrum of the background contained in that same slice. The presented spectrum corresponds to the average of the division products over all slices. The absorption lines identified upon visual inspection of the spectrum have been marked:  $^{12}\text{C}^{16}\text{O}_2$  (yellow),  $^{13}\text{C}^{16}\text{O}_2$  (red),  $^{12}\text{C}^{16}\text{O}$  (dark blue).

The observation of weak  $\text{CO}_2$  absorption lines has been suggested as an observational discriminant of a Venus-like environment in telluric exoplanets [12]. This is associated with the high abundance of  $\text{CO}_2$  implied for the observed atmosphere by the presence of these weaker lines. While the observation of strong  $\text{CO}_2$  bands (e.g.,  $4.3\ \mu\text{m}$ ) in transmission spectra suggests the detection of an atmosphere for terrestrial exoplanets, the inherently higher probability for these electronic transitions to take place

turns their detection insufficient to discriminate between a CO<sub>2</sub> dominated environment and one with trace amounts of this gas. The detection of weak absorption features in the retrieved transmission spectrum of Venus corroborates this hypothesis.

Furthermore, the extracted spectrum comprises a unique template with enhanced S/N of what a Venus-like exoplanetary atmosphere should look like when observed by NIR high-dispersion spectrographs.

#### 4.2. Cross-Correlation Analysis

The resulting CCFs in Venus rest frame are shown in Figure 4, alongside the best-fit Gaussian profiles. Table 2 shows a list of the species with tentative absorption features identified in the CCFs, alongside the best-fit values from the Gaussian fit parameters (amplitude, centre radial velocity and FWHM) and associated uncertainties. To measure the significance of the observed signals in the CCFs we calculated the ratio of the fit amplitude to the standard deviation of the out-of-peak continuum, where the cross-correlation function is expected to be dominated by noise. We define out-of-peak continuum regions between  $[-30, -100]$  km s<sup>-1</sup> and  $[+30, +100]$  km s<sup>-1</sup>.

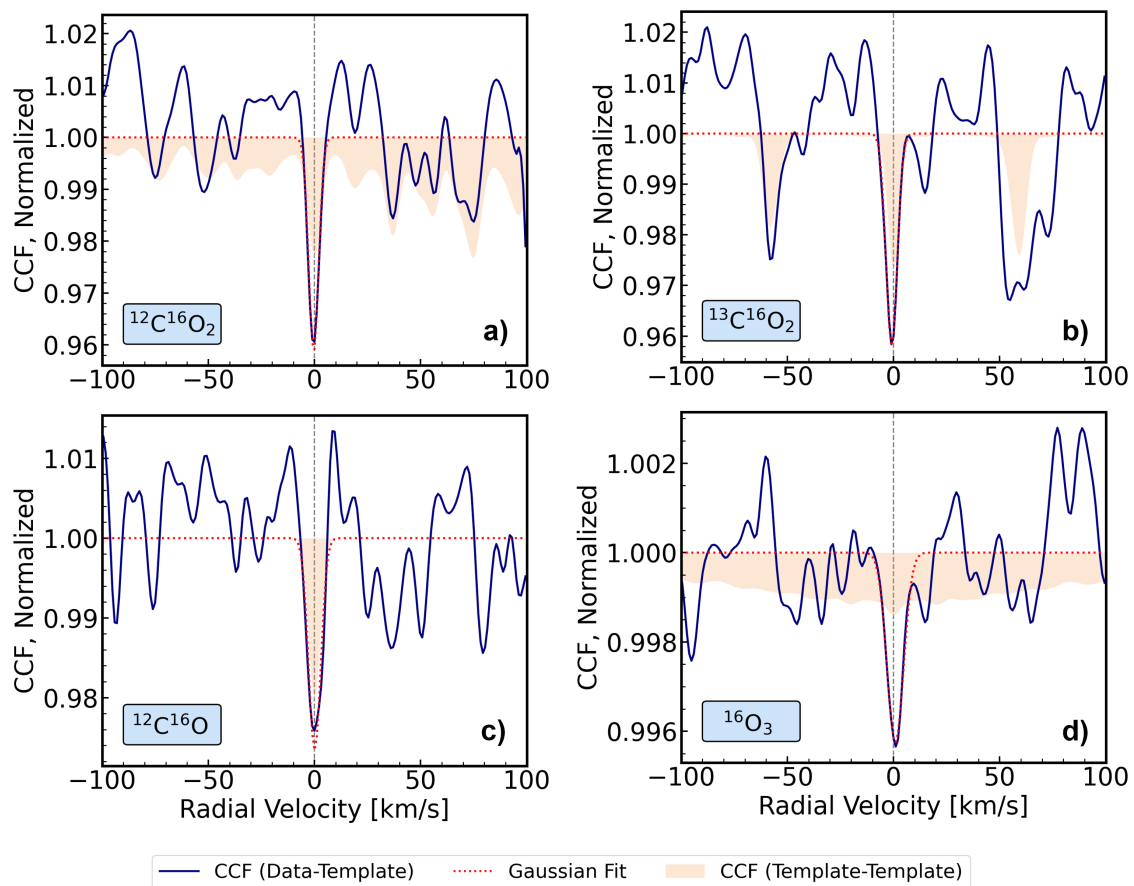


**Figure 4.** Cross-correlation functions for (a)  $^{12}\text{C}^{16}\text{O}_2$ , (b)  $^{13}\text{C}^{16}\text{O}_2$ , (c)  $^{12}\text{C}^{16}\text{O}$  and (d)  $^{16}\text{O}_3$  (dark blue line). The best-fit Gaussian profiles are shown for each CCF (red dashed line). All panels show the CCFs resulting from the self cross-correlation of the templates (light orange area), which are scaled arbitrarily.

For CO<sub>2</sub>, it was possible to reveal CCF signals for the two most abundant isotopologues. For the main isotopologue,  $^{12}\text{C}^{16}\text{O}_2$ , we find an absorption signal with a significance of  $4.2\sigma$ . Our analysis for  $^{13}\text{C}^{16}\text{O}_2$  has revealed a central peak, at  $-0.88 \pm 0.56$  km s<sup>-1</sup>, but also two secondary peaks at about  $-60$  km s<sup>-1</sup> and  $+60$  km s<sup>-1</sup>, which also appear significant.



To address the significance of the main peak we studied the origin of these secondary peaks on the CCF. For that, we cross-correlated the transmission model for  $^{13}\text{C}^{16}\text{O}_2$  with itself at the same spectral resolution as the observations. The result of the template-template CCF is shown in orange in Figure 4. The template-template CCF shows the expected signal at  $0\text{ km s}^{-1}$ , but also two symmetric peaks at RV similar to the ones present in the Data-Template CCF. These peaks can be expected due to the periodicity in the distribution of lines in the spectrum of this isotopologue. The presence of the secondary peaks in the Data-Template and Template-Template CCFs strengthens the detection of  $^{13}\text{C}^{16}\text{O}_2$  in the transmission spectrum of Venus [28]. In this context, we masked the intervals of RV between  $[-40, -70]\text{ km s}^{-1}$  and  $[+40, +70]\text{ km s}^{-1}$  when measuring the significance of the main peak for  $^{13}\text{C}^{16}\text{O}_2$ , which was estimated to be  $4.7\sigma$ .

We note that we have calculated template-template cross-correlations for the other species detected (see Figure 4). Nonetheless, these secondary signals do not result in relevant peaks in the rest of our CCFs, apart from  $^{13}\text{C}^{16}\text{O}_2$ , which made us only account for these effects when estimating the significance of this detection.

Additionally, the CCF analysis enabled the detection of the main isotopologue of CO in Venus upper atmosphere, with a significance of  $3.9\sigma$ . On Venus atmosphere, CO comprises a photolytic by-product of  $\text{CO}_2$ , which has been regarded as an indicator of atmospheric desiccation for atmospheres of rocky exoplanets [12]. This is because photolytic by-products of  $\text{H}_2\text{O}$ , such as hydroxyl radicals, act as catalysts in the chemical reaction between CO and free oxygen, resulting in the production of  $\text{CO}_2$  [29].

**Table 2.** Summary of the Gaussian fit parameters for the detected species in the transmission spectrum of Venus.

Molecule	Amplitude [ppm]	Center RV [km s <sup>-1</sup> ]	FWHM [km s <sup>-1</sup> ]	S/N [σ]
$^{12}\text{C}^{16}\text{O}_2$	$41293 \pm 5698$	$-0.36 \pm 0.37$	$5.52 \pm 0.88$	4.2
$^{13}\text{C}^{16}\text{O}_2$	$42048 \pm 7765$	$-0.88 \pm 0.56$	$6.2 \pm 1.3$	4.7
$^{12}\text{C}^{16}\text{O}$	$26558 \pm 3727$	$0.089 \pm 0.465$	$6.8 \pm 1.1$	3.9
$^{16}\text{O}_3$	$4244 \pm 512$	$0.85 \pm 0.54$	$9.2 \pm 1.3$	3.5

Furthermore, we also report the detection of the main isotopologue of  $\text{O}_3$  with a significance of  $3.5\sigma$ . Our result follows previous detections of ozone in the upper atmosphere of Venus in the ultra-violet (UV) domain [19,30]. However, the detection here reported comprises the first observation of  $\text{O}_3$  on the planet in the NIR and using ground-based instrumentation.

Similarly to CO,  $\text{O}_3$  is produced from  $\text{CO}_2$  photolysis on Venus upper atmosphere [19]. Its abiotic origin on Venus contrasts with the important role of biological photosynthesis in the accumulation of this gas on Earth’s atmosphere. Ultimately, this result demonstrates how  $\text{O}_3$  can lead to potential false positives in biosignature detections in telluric exoplanets.

Atmospheric  $\text{O}_3$  has also been proposed as an indicator of atmospheric desiccation for rocky planets, given it reacts with photolytic by-products of  $\text{H}_2\text{O}$  [29]. Particularly, the detection of large amounts of atmospheric CO in the presence of  $\text{O}_3$  should constitute a false positive in biosignature search, since the high abundance of CO suggests that  $\text{O}_3$  is more likely to have been produced from  $\text{CO}_2$  photolysis, and not from biological activity [12].

5. Conclusions

We report the detections of  $^{12}\text{C}^{16}\text{O}_2$ ,  $^{13}\text{C}^{16}\text{O}_2$ ,  $^{12}\text{C}^{16}\text{O}$  and  $^{16}\text{O}_3$  in the high-resolution transmission spectrum of Venus as observed with DST-FIRS during the solar transit of 2012. The reported detection significance cannot be used to estimate the atmospheric abundances of the said species, given these are relative to baseline regions of the CCF.

Our result confirms the detection of O<sub>3</sub> in the upper atmosphere of Venus, showcasing how high-resolution, ground-based, NIR observations are effective at detecting this gas in planetary atmospheres. This detection combined with the detection of CO reinforces the role of these species as indicators of dry, Venus-like climates.

On Earth, the formation pathway of O<sub>3</sub> is intimately connected with production of O<sub>2</sub> from biological activity, resulting in the contemplation of O<sub>3</sub> as a tentative biosignature gas in exoplanetary atmospheres. In this context, our result contributes to contextualize future detections of atmospheric ozone in high-resolution studies of rocky exoplanets. Eventually, some of these detections can pertain to Venus-like environments, where abiotic production mechanisms are likely to be also operating.

Furthermore, our high-resolution NIR observations in the 1.5  $\mu\text{m}$  band have been able to resolve absorption lines from the two most abundant isotopes of CO<sub>2</sub>. These spectral lines comprise particularly weak spectral features of CO<sub>2</sub> in comparison with strong carbon dioxide bands (e.g., 4.3  $\mu\text{m}$ ). The observation of weak absorption bands of this greenhouse gas has been contemplated as an important indicator of a Venus-like abundance of CO<sub>2</sub>, which can facilitate the characterization of rocky exoplanets with Venus-like environments. We show the potential of the transmission spectroscopy technique to observe these absorption features in the NIR using high-resolution spectrographs.

We highlight the capability of the cross-correlation technique to differentiate between distinct isotopologues of carbon dioxide present in the retrieved planetary spectra. The detection of atmospheric isotopologues in Earth-sized exoplanets, alongside the subsequent computation of isotopic ratios, comprises a valuable tool to study formation and evolutionary mechanisms in distant telluric worlds, and would ultimately provide valuable insights into the evolution and diversity of planetary systems.

Currently it is not possible to resolve exoplanets in front of their host star as in the case of the transit of Venus here analysed. Consequently, the reported method used to retrieve the transmission spectrum of Venus differs from that involved in retrieving atmospheric transmission spectra of an exoplanet. Nonetheless, the observations of the Venus solar transit analysed in this study demonstrate the potential of this technique. With the development of future high-resolution spectrographs for the Extremely Large Telescope (e.g., ANDES; [31]), this method could be widely applied. In that context, atmospheric observables identified for Venus should be critical to differentiate between Earth- and Venus-analogues.

**Author Contributions:** Conceptualization, A.B. and P.M.; methodology, A.B., P.M., O.D. and S.J.; software, A.B. and P.M.; validation, P.M. and O.D.; formal analysis, A.B., P.M. and S.J.; investigation, A.B., P.M., O.D., S.J., T.W. and P.T.; resources, A.B., P.M., O.D., S.J., T.W. and P.T.; data curation, A.B., S.J.; writing—original draft preparation, A.B. and P.M.; writing—review and editing, A.B., P.M. and O.D.; visualization, A.B., P.M., O.D., S.J., T.W. and P.T.; supervision, P.M. and O.D. All authors have read and agreed to the published version of the manuscript.

**Funding:** This research received no external funding.

**Data Availability Statement:** The raw data supporting the conclusions of this article will be made available by the authors, without undue reservation.

**Acknowledgments:** This work was supported by the Portuguese Fundação para a Ciência e a Tecnologia of reference PTDC/FIS-AST/29942/2017, through national funds and by FEDER through COMPETE 2020 of reference POCI-01-0145- FEDER-007672.

**Conflicts of Interest:** The authors declare no conflicts of interest.

## Abbreviations

The following abbreviations are used in this manuscript:

NIR	Near-Infrared
FIRS	Facility Infrared Spectropolarimeter
DST	Dunn Solar Telescope
ELT	Extremely Large Telescope
ARIEL	Atmospheric Remote-sensing Infrared Exoplanet Large-survey
HITRAN	High-Resolution Transmission Molecular Absorption Database
VIRA	Venus International Reference Atmosphere
DACE	Data Analysis Centre for Exoplanets
CCF	Cross-Correlation Function
RV	Radial Velocity
FWHM	Full Width at Half Maximum
SPICAV	Spectroscopy for Investigation of Characteristics of the Atmosphere of Venus
SOIR	Solar Occultation at Infrared

## Appendix A

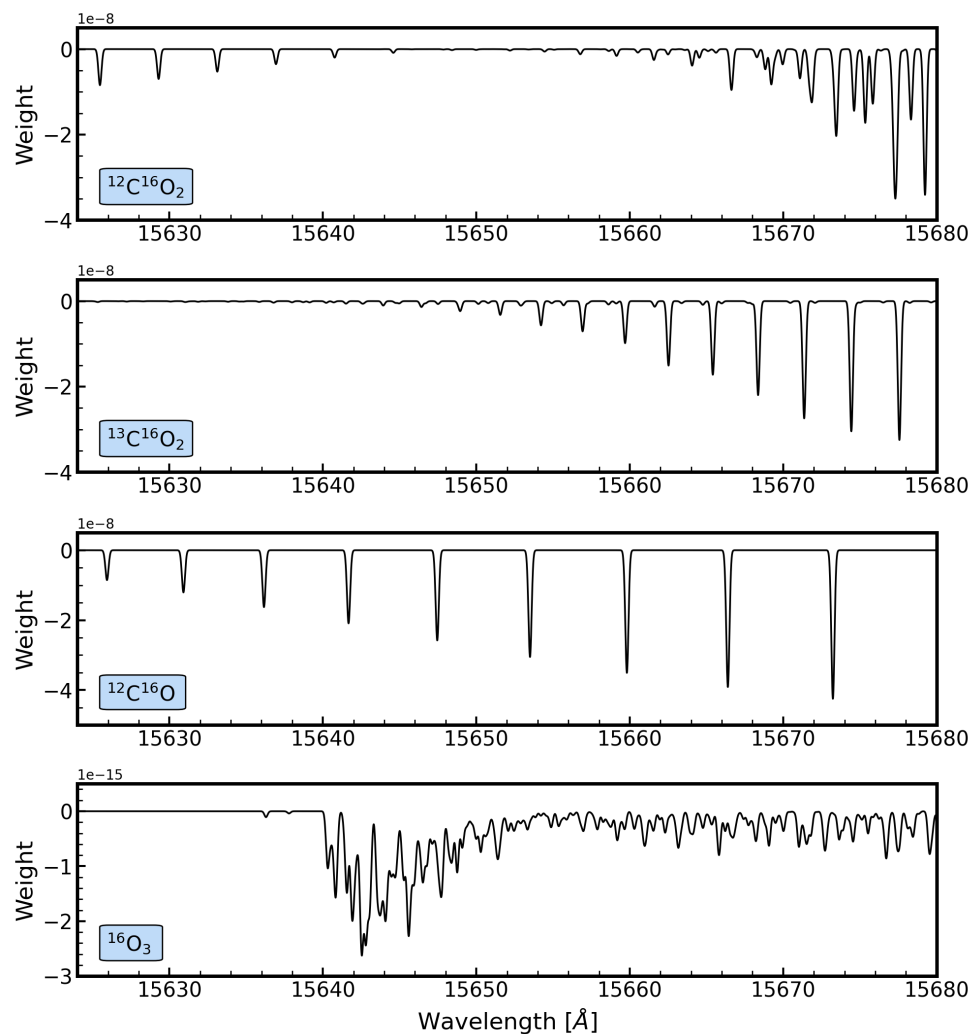


**Figure A1.** Transmission templates used in cross-correlation analysis for each chemical specie. The results we present for each species use an isothermal PT profile at 175 K.

## References

1. William, S.; Sanjay, S. *Venus*, 1st ed.; Reaktion Books: London, England, 2022; pp. 44–61.
2. Ehrenreich, D.; Vidal-Madjar, A.; Widemann, T.; Gronoff, G.; Tanga, P.; Barthélemy, M.; Lilensten, J.; Lecavelier Des Etangs, A.; Arnold, L. Transmission spectrum of Venus as a transiting exoplanet. *Astron. Astrophys.* **2012**, *537*, L2, DOI
3. Reale, F.; Gambino, A.; Micela, G.; Maggio, A.; Widemann, T.; Piccioni, G. Using the transit of Venus to probe the upper planetary atmosphere. *Nat. Commun.* **2015**, *6*, 7563, DOI
4. Azevedo Silva, T.; Demangeon, O.; Santos, N.; Allart, R.; Borsa, F.; Cristo, E.; Esparza-Borges, E.; Seidel, J.; Palle, E.; Sousa, S.; et al. Detection of barium in the atmospheres of the ultra-hot gas giants WASP-76b and WASP-121b. Together with new detections of Co and Sr+ on WASP-121b. *Astron. Astrophys.* **2022**, *666*, L10, DOI
5. Snellen, I.; de Kok, R.; de Mooij, E.; Albrecht, S. The orbital motion, absolute mass and high-altitude winds of exoplanet HD209458b. *Nature* **2010**, *465*, 1049–1051, DOI
6. Seidel, J.; Prinoth, B.; Knudstrup, E.; Hoeijmakers, H.; Zanazzi, J.; Albrecht, S. Detection of atmospheric species and dynamics in the bloated hot Jupiter WASP-172 b with ESPRESSO. *Astron. Astrophys.* **2023**, *678*, A150, DOI
7. Madhusudhan, N.; Sarkar, S.; Constantinou, S.; Holmberg, M.; Piette, A.; Moses, J. Carbon-bearing Molecules in a Possible Hycean Atmosphere. *Astrophys. J. Lett.* **2023**, *956*, L13, DOI
8. Lustig-Yaeger, J.; Meadows, V.; Lincowski, A. The Detectability and Characterization of the TRAPPIST-1 Exoplanet Atmospheres with JWST. *Astron. J.* **2019**, *158*, 27, DOI
9. Ehrenreich, D.; Tinetti, G.; Lecavelier Des Etangs, A.; Vidal-Madjar, A.; Selsis, F. The transmission spectrum of Earth-size transiting planets. *Astron. Astrophys.* **2006**, *228*, 379–393, DOI
10. Kane, S.; Barclay, T.; Gelino, D. A potential super-Venus in the Kepler-69 System. *Astrophys. J. Lett.* **2013**, *770*, L20, DOI
11. Hedelt, P.; Alonso, R.; Brown, T.; Collados Vera, M.; Rauer, H.; Schleicher, H.; Schmidt, W.; Schreier, F.; Titz, R. Venus transit 2004: Illustrating the capability of exoplanet transmission spectroscopy. *Astron. Astrophys.* **2011**, *533*, A136, DOI
12. Lincowski, A.; Meadows, V.; Crisp, D.; Robinson, T.; Luger, R.; Lustig-Yaeger, J.; Arney, G. Evolved Climates and Observational Discriminants for the TRAPPIST-1 Planetary System. *Astrophys. J.* **2018**, *867*, 76, DOI
13. Pere, C.; Tanga, P.; Widemann, T.; Bendjoya, P.; Mahieux, A.; Wilquet, V.; Vandaele, A. Multilayer modeling of the aureole photometry during the Venus transit: comparison between SDO/HMI and VEx/SOIR data. *Astron. Astrophys.* **2016**, *595*, A115, DOI
14. Jaeggli, S.; Reardon, K.; Pasachoff, J.; Schneider, G.; Widemann, T.; Tanga, P. 1565 nm Observations of the transit of Venus, Proxy for a Transiting Exoplanet. *AAS/Sol. Phys. Div. Meet.* **2013**, *44*, 100.150
15. Mollière, P.; Wardenier, J.; van Boekel, R.; Henning, Th.; Molaverdikhani, K.; Snellen, I. petitRADTRANS. A Python radiative transfer package for exoplanet characterization and retrieval. *Astron. Astrophys.* **2019**, *267*, A67, DOI
16. Gruchola, S.; Galli, A.; Vorburger, A.; Wurz, P. The upper atmosphere of Venus: Model predictions for mass spectrometry measurements. *Planet. Space Sci.* **2019**, *170*, 29–41, DOI
17. Keating, G.; Bertaux, J.; Bougher, S.; Dickinson, R.; Cravens, T.; Nagy, A.; Hedin, A.; Krasnopolsky, V.; Nicholson III, J.; Paxton, L.; von Zahn, U. Models of Venus neutral upper atmosphere: Structure and composition. *Adv. Space Res.* **1985**, *5*, 117–171, DOI
18. Seiff, A.; Schofield, J.; Kliore, A.; Taylor, F.; Limaye, S.; Revercomb, H.; Sromovsky, L.; Kerzhanovich, V.; Moroz, V.; Marov, M. Models of the structure of the atmosphere of Venus from the surface to 100 kilometers altitude. *Adv. Space Res.* **1985**, *5*, 3–58, DOI
19. Montmessin, F.; Bertaux, J.; Lefèvre, F.; Marcq, E.; Belyaev, D.; Gérard, J.; Korabiev, O.; Fedorova, A.; Sarago, V.; Vandaele, A. A layer of ozone detected in the nightside upper atmosphere of Venus. *Icarus* **2011**, *216*, 82–85, DOI
20. Grimm, S.; Malik, M.; Kitzmann, D.; Guzmán-Mesa, A.; Hoeijmakers, H.; Fisher, C.; Mendonça, J.; Yurchenko, S.; Tennyson, J.; Alesina, F.; et al. HELIOS-K 2.0 Opacity Calculator and Open-source Opacity Database for Exoplanetary Atmospheres. *Astrophys. J. Suppl. Ser.* **2021**, *253*, 30, DOI

21. Esposito, L.; Knollenberg, R.; Marov, M.; Toon, O.; Turco, R. The clouds and hazes of Venus. In *Venus*; Hunten, D., Colin, L., Donahue, T., Moroz, V., Eds.; The University of Arizona Press: Tucson, AZ, 1983; pp. 484–564
22. Roos, M.; Drossart, P.; Encrenaz, T.; Lellouch, E.; Bézard, B.; Carlson, R.; Baines, K.; Kamp, L.; Taylor, F.; Collard, A.; et al. The upper clouds of Venus: determination of the scale height from NIMS-Galileo infrared data. *Planet. Space Sci.* **1993**, *41*, 505–514, [DOI](#)
23. Grinspoon, D.; Pollack, J.; Sitton, B.; Carlson, R.; Kamp, L.; Baines, K.; Encrenaz, T.; Taylor, F. Probing Venus's cloud structure with Galileo NIMS. *Planet. Space Sci.* **1993**, *41*, 515–542, [DOI](#)
24. Wilquet, V.; Fedorova, A.; Montmessin, F.; Drummond, R.; Mahieux, A.; Vandaele, A.; Villard, E.; Korabiev, O.; Bertaux, J. Preliminary characterization of the upper haze by SPICAV/SOIR solar occultation in UV to mid-IR onboard Venus Express. *J. Geophys. Res. Planets* **2009**, *114*, E00B42, [DOI](#)
25. Virtanen, P.; Gommers, R.; Oliphant, T.; Haberland, M.; Reddy, T.; Cournapeau, D.; Burovski, E.; Peterson, P.; Weckesser, W.; Bright, J.; et al. SciPy 1.0: fundamental algorithms for scientific computing in Python. *Nat. Methods* **2020**, *17*, 261–272, [DOI](#)
26. Newville, M.; Stensitzki, T.; Allen, D.; Rawlik, M.; Ingargiola, A.; Nelson, A. Lmfit: Non-Linear Least-Square Minimization and Curve-Fitting for Python. *Astrophysics Source Code Library* **2016**, [DOI](#)
27. Gordon, I.; Rothman, L.; Hargreaves, R.; Hashemi, R.; Karlovets, E.; Skinner, F.; Conway, E.; Hill, C.; Kochanov, R.; Tan, Y.; Wcisło, P.; et al. The HITRAN2020 molecular spectroscopic database. *J. Quant. Spectrosc. Radiat. Transfer* **2022**, *277*, 107949, [DOI](#)
28. Esparza-Borges, E.; López-Morales, M.; Adams Redai, J.; Pallé, E.; Kirk, J.; Casasayas-Barris, N.; Batalha, N.; Rackham, B.; Bean, J.; Casewell, S.; et al. Detection of Carbon Monoxide in the Atmosphere of WASP-39b Applying Standard Cross-correlation Techniques to JWST NIRSpec G395H Data. *Astrophys. J. Lett.* **2023**, *955*, L19, [DOI](#)
29. Gao, P.; Hu, R.; Robinson, T.; Li, C.; Yung, Y. Stability of CO<sub>2</sub> Atmospheres on Desiccated M Dwarf Exoplanets. *Astrophys. J.* **2015**, *806*, 249, [DOI](#)
30. Marcq, E.; Baggio, L.; Lefèvre, F.; Stolzenbach, A.; Montmessin, F.; Belyaev, D.; Korabiev, O.; Bertaux, J. Discovery of cloud top ozone on Venus. *Icarus* **2019**, *319*, 491–498, [DOI](#)
31. Palle, E.; Biazio, K.; Bolmont, E.; Molliere, P.; Poppenhaeger, K.; Birkby, J.; Brogi, M.; Chauvin, G.; Chiavassa, A.; Hoeijmakers, J.; et al. Ground-breaking Exoplanet Science with the ANDES spectrograph at the ELT. *arXiv e-prints* **2023**, arXiv:2311.17075, [DOI](#)

**Disclaimer/Publisher's Note:** The statements, opinions and data contained in all publications are solely those of the individual author(s) and contributor(s) and not of MDPI and/or the editor(s). MDPI and/or the editor(s) disclaim responsibility for any injury to people or property resulting from any ideas, methods, instructions or products referred to in the content.